Pure & Appl. Chem., Vol. 56, No. 2, pp. 189-208, 1984.
Printed in Great Britain.

0033-4545/84 $3.00+0.00
Pergamon Press Ltd.

Optical Techniques in Plasma Diagnostics

Richard A. Gottscho
Terry A. Miller

Bell Laboratories
Murray Hill, New Jersey 07974

ABSTRACT

Recent developments in optical techniques for plasma diagnostics are critically reviewed. The primary emphasis is on plasma-induced emission and laser-induced fluorescence probes of radical and ionic concentrations and temperatures in low pressure discharges like those used in microelectronic fabrication. Other techniques such as optogalvanic, infrared, spontaneous and stimulated Raman, and multiphoton spectroscopy are also discussed briefly.

Generally, emission techniques are seen to be useful primarily for qualitative analysis and characterization of the electron energy distribution. However, in some systems, emission actinometry, where an inert gas is used to account for changes in electron density, appears to be a valid means of determining relative changes in concentration. Laser-induced fluorescence spectroscopy has only recently been utilized for *in situ* measurements of ground state ions and radicals but has already yielded insight into mechanisms for formation, destruction, energy transfer, and maintenance of the discharge. By and large the other techniques show great promise but remain to be exploited as diagnostic tools for plasmas.

I. INTRODUCTION

Diagnostic techniques for plasmas have shared in the growth in interest and popularity that the general field of plasma chemistry and processing has recently enjoyed. This is true even though the goal of plasma diagnostics is the basic understanding of plasma chemistry and related phenomena, rather than the production of an economically viable device or material. The key to this overall interest is that the success of a particular process leading to a desired product can often depend critically on the delicate balancing of numerous factors inherent in the plasma. For example in the production of micro-electronic devices, factors that must be considered include, surface bombardment by positive ions - their energy and directionality, availability of neutral reactive species, production and destruction of surface films on wafers, etc.

For most plasma processes a number of variables, e.g. gas mixture, gas flow, rf power, etc., can be externally controlled to optimize the balance between competing chemical and physical processes. However the number of variables available is so large that the employment of a random sampling technique to achieve optimization of reactor conditions for a given process would place severe demands upon the patience of any investigator. For this reason it is important to develop reliable diagnostic tools, both to provide a basic understanding of the plasma and to serve as useful indicators for actual processes.

It may be convenient to divide diagnostic techniques into three general categories, *ex situ*, *in situ*-intrustive, *in situ*-non-intrustive. The common characteristic of *ex situ* techniques is that they sample an aliquot of the plasma reactor's contents and transfer it elsewhere for examination. Analytical techniques that have been employed in this manner are mass-spectrometry, gas-phase electron paramagnetic resonance, gas chromatography, and chemical titrations via downstream reactions. The advantage of the *ex situ* techniques is that they allow the full power of numerous analytical techniques to be employed. The chief disadvantage of *ex situ* techniques is fairly obviously. Since the contents of a plasma reactor encompass many highly reactive species, ions, free radicals, reactive atoms, one can never be certain that species analyzed *ex situ* have not been transmuted during their journey from the reactor.

The division of *in situ* techniques into intrustive and non-intrustive is somewhat arbitrary. To some extent, any diagnostic technique perturbs the plasma. However, in some cases this perturbation may be so slight as to be negligible, while in others it may be quite considerable. One example of an *in situ*

diagnostic which would generally be called intrustive is a Langmuir probe. Clearly in this case one is inserting a physical object into the medium and thereby perturbing it. However, depending upon the information desired this perturbation may or may not be negligible.

Almost certainly the least intrustive *in situ* diagnostics yet developed use photons as the information transmitter between the medium and the observer. Rarely will they perturb the medium in a non-negligible manner. Such photon-driven diagnostics, conveniently called optical diagnostic even though the photons involved may be outside the spectral region visible to the human eye, will be the subject of the remainder of this paper. We will review early optical diagnostic work which consisted mainly of an analysis of the optical emission generated by the plasma itself. We will discuss attempts to make this technique more quantitative by the use of actinometers. The success and limitations of actinometric techniques are considered.

We also discuss laser induced fluorescence diagnostics of plasma systems. We consider some of the advantages of laser induced fluorescence especially in the areas of high spatial and temporal resolution, and quantitative analysis, and we illustrate the kinds of plasma information obtainable from such techniques by the use of specific examples.

We will also touch upon some of the other "optical" techniques that have possible application for plasma diagnostics. These include opto-galvanic techniques, IR emission and absorption including laser techniques, Raman scattering, and multi-photon excitation. We conclude with a short summary and a look towards future applications. This paper is written from the optical diagnostic or spectroscopic point of view. In this sense, the techniques described could be applied to either a thermal plasma or a non-equilibrium plasma. Our own work is in the non-equilibrium plasma area and it is for this reason that the examples we cite are from this area.

II. EMISSION SPECTROSCOPY DIAGNOSTICS

Most plasma reactors give off a variety of "optical" emissions ranging throughout the spectrum from the IR to the UV. One of the simplest diagnostics for plasmas is the spectral analysis of this radiation. Usually this is accomplished by passing the emission through a monochromator and recording its time averaged spectral features. It is convenient to illustrate the advantages and limitations of emission diagnostics by recounting the history of its application to one of the most widely studied plasma systems, the etching of Si and SiO_2 by a CF_4-O_2 plasma.

A. CF_4-O_2 Emission

A little over 5 years ago, Harshbarger, Porter, Miller, and Norton (1) undertook a simple study of the resolved emission from a standard parallel plate plasma reactor etching Si with a mixture of CF_4-O_2. Fig. 1 shows a typical emission spectrum recorded with Si wafers present (bottom) and absent (top). As

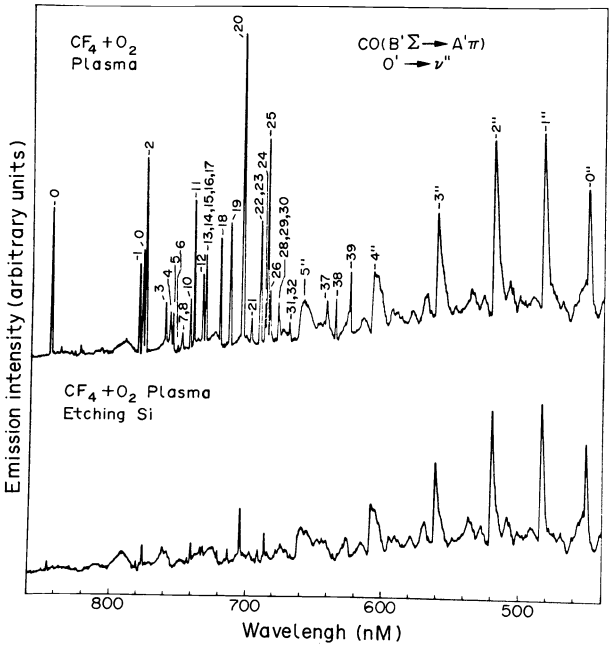

Fig. 1. Emission spectrum of CF_4-O_2 plasma. Bottom trace Si wafers present, top trace absent.

Fig. 1 shows, the three principal species emitting from the CF_4-O_2 plasma are F and O atoms and the CO molecule. The trace with Si wafers shows drastically less atomic emission but comparable CO emission. From this evidence alone, one would likely conclude that the F and O atoms are active in the etching process but CO is not.

In Fig. 2 we have plotted the F atom emission, the O atom emission and the Si etch rate vs. O_2 concentration. We note that the F atom emission and etch rate are strongly correlated but do not have an identical functional form. The O atom emission shows little direct relationship with the Si etch rate, but increases rapidly as a function of O_2 once the maximum in the Si etch rate is reached. A model qualitatively consistent with the above data can be drawn as follows. F atoms are the active species etching Si. When small amounts of O_2 are added to the discharge, chemical reactions involving O_2 and/or O atoms liberate more F atoms, which results in an increase in the etch rate. The reaction of O atoms with some species in the reactor controls the concentration of O atom emission, till a point near the maximum Si etch rate when this reaction is no longer efficient enough to prevent a rapid increase in O atom emission.

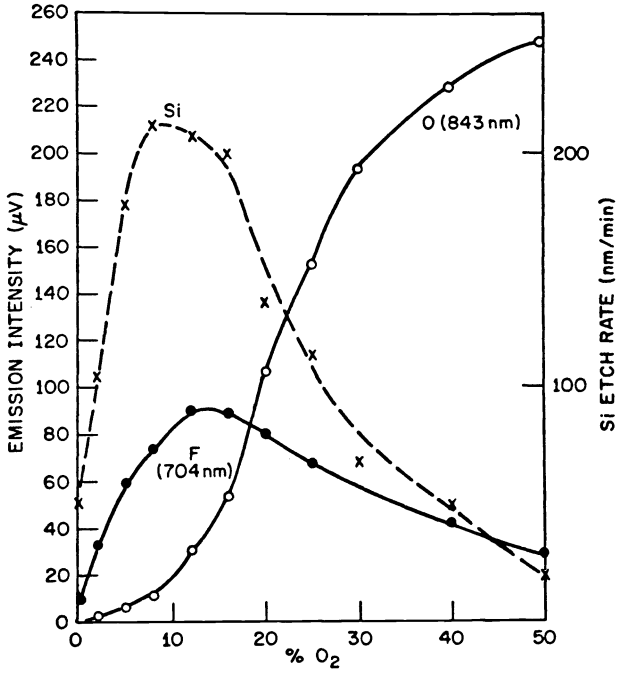

Fig. 2. F, O emission, etch rate vs. O_2 addition (see Ref. 1).

These qualitative conclusions based upon the simple emission diagnostics are all still believed to be qualitatively correct, but they are not the whole story. For instance, Mogab, Adams and Flamm (2,3) carried out a more detailed investigation of the CF_4-O_2 etching of Si and confirmed that while the curves giving F atom emission and Si etching vs. O_2 concentration are similar, they are certainly not identical. This result is not consistent with the assumptions that (i) the emission intensity, I_F, is proportional to the F atom concentration [F] and (ii) that the etch rate R is proportional to [F]. For then

$$R = (\beta_F/\alpha_F^e)\, I_F \tag{1}$$

where

$$R = \beta_F[F] \tag{2a}$$

with β_F = proportionality constant relating R and [F] and

$$[F] = I_F/\alpha_F^e \tag{2b}$$

with α_F^e = proportionality constant relating I_F and [F].

Let's first consider the assumption that I_F and [F] are proportional, by examining the proportionality constant α_F^e in more detail,

$$\alpha_F^e = K \int_0^\infty Q(P, N_e)\ \sigma_F^e(\epsilon)\ N_e(\epsilon)\, d\epsilon \tag{3}$$

where

K = a constant depending on the sensitivity of the detector.

$\sigma_F^e(\epsilon)$ = cross-section for excitation of the emitting species (F atoms) to a given excited state by impact of an electron of energy ϵ.

$N_e(\epsilon)$ = number of electrons in the energy range $d\epsilon$ present in the volume of the reactor viewed by the detector.

$Q(P, N_e)$ = quantum yield for emission from the given excited state of interest as a function of discharge pressure and electron density.
In principle Q varies between 0 and 1.

When one looks at the factor α_F^e in this manner, it is obvious that it is anything but a constant. In fact it is remarkable that an equation like (2b) has any usefulness at all. Rigorously speaking, the number density of electrons as a function of energy and the quantum yield must be invariant for the emission and concentration to be simply related. Since $N_e(\epsilon)$ depends on applied RF power and gas mixture and Q depends on total pressure and gas mixture, α_F^e will never be precisely a constant. Furthermore Eq. 3 assumes that all the F emission originates from excitation of ground state F atoms. If other processes contribute to I_F, e.g. $CF_4 + e^- \rightarrow CF_3 + F^*$, then Eq. 2b is totally invalid.

However in some cases of practical interest things may be somewhat better than indicated above. For plasma etching applications, the pressure and electron density are relatively low, thus $Q(P, N_e)$ may be very nearly unity over a range of operating conditions, especially for short-lived excited states. Similarly $\sigma^e(\epsilon)$ may be a relatively "slow" function of ϵ, and $N^e(\epsilon)$ may not depend extremely strongly on gas composition. Nonetheless, variations in α due to these considerations are nearly impossible to avoid. Similar, but more difficult-to-estimate, are the errors likely introduced by processes contributing to I_F, other than ground state F atom concentration excitation.

In the work of Mogab, et al., (2) an effort was made to measure the variation of α_F^e as a function of O_2 addition to the discharge. For this experiment an independent method for [F] determination is required and these workers employed a downstream chemical titration of F atoms. Such an *ex situ* technique eliminates the possibility of an absolute calculation for α_F^e, but barring some chemical pathologies, it is plausible to assume that the relative variation of α_F^e with varying O_2 concentrations can be measured. The results of these experiments are shown in Fig. 3.

The value of α_F^e can be seen to vary by over a factor of two for a reasonable range of O_2 addition. While this change is quite modest compared to what could be expected from an analysis of Eq. 3 it is comparable to the deviation between the I_F curve and etch rate curve vs. O_2 concentration. Unfortunately this variation in α_F^e is precisely in the *wrong* direction to make the I_F and R curves coincide!

Thus there must be something more complicated in the etching mechanism, requiring more than the simple relation Eq. 2a between etching and F atom concentration. It has been proposed (2) that besides its role in liberating more F atoms to etch, O_2 addition produces O atoms which compete with F atoms for surface sites. When O atom concentrations become significant, such competition can decrease the overall etching rate. Quantitatively then

$$R = \beta[F]^2/([F] + k[O]) \tag{4}$$

where k gives the competitive efficiency for O vs. F atoms. It is found that by using I_F, I_O and the experimentally determined variation of α_F^e, the etch rate R can be correctly predicted by Eq. (4) over a wide range of O_2 concentrations (2).

The moral of the story is that plasma mechanisms can be complex and reliable diagnostics are absolutely necessary if one is to even hope for an understanding of them. Simple emission spectroscopy is a good qualitative tool, but great care must be exercised in its quantitative application.

B. Actinometry

The non-constancy of α_F^e in Eqs. (1) and (2b) is quite troubling. In the above CF_4-O_2 example, the variation in α_F^e was determined by an *ex situ* chemical titration, hardly a universal solution. A more

general approach to this problem has been the development of actinometry. In this case one monitors not only the emission I_r^e from the reactive species of interest, but also the fluorescence, I_i^e of an inert gas, e.g. Ar or N_2, in the same plasma. Then we have

$$I_r^e/I_i^e = (N_r/N_i)(\alpha_r^e/\alpha_i^e) = (N_r/N_i) \times$$

$$\left[\frac{\int_0^\infty Q_r(P,N_e)\,\sigma_r^e(\epsilon)\,N_e(\epsilon)\,d\epsilon}{\int_0^\infty Q_i(P,N_e)\,\sigma_i^e(\epsilon)\,N_e(\epsilon)\,d\epsilon}\right] \tag{5a}$$

It is clear that if the bracketed integrals are equivalent, then one has a very simple result. The requirement for this equivalency is that the quantum yield and the cross sections have the same energy dependence. Since for short-lived excited states in a low pressure cold plasma Q is essentially unity, this requirement simply reduces to one on the cross section. In no case will two different species have exactly the same functional form for the energy dependence of the cross section, but if the actinometer species is wisely chosen, the form of $\sigma_r^e(\epsilon)$ and $\sigma_i^e(\epsilon)$ may be similar enough to give practical results of considerable utility.

Coburn and Chen (4) tested the actinometric technique by monitoring I_F^e/I_{Ar}^e in $CF_4/O_2/Ar$ plasmas as a function of the O_2 feedstock composition. They found excellent agreement between I_{Ar}^e and α_F^e, determined previously by Mogab *et al.* (2) (Fig. 3). Thus, Eqn. (5a) simplifies to

$$I_F^e/I_{Ar}^e = K N_F/N_{Ar} \tag{5b}$$

where K is a constant. Ar satisfies at least two key actinometric criteria: it is relatively inert and the excited state involved lies at ~13.5 eV compared to ~14.5 eV for the corresponding F state. Although the technique appears to work well in this case, the origin of the F atom emission was not determined; so, the question lingers as to whether or not the agreement observed by Coburn and Chen (4) was merely fortuitous.

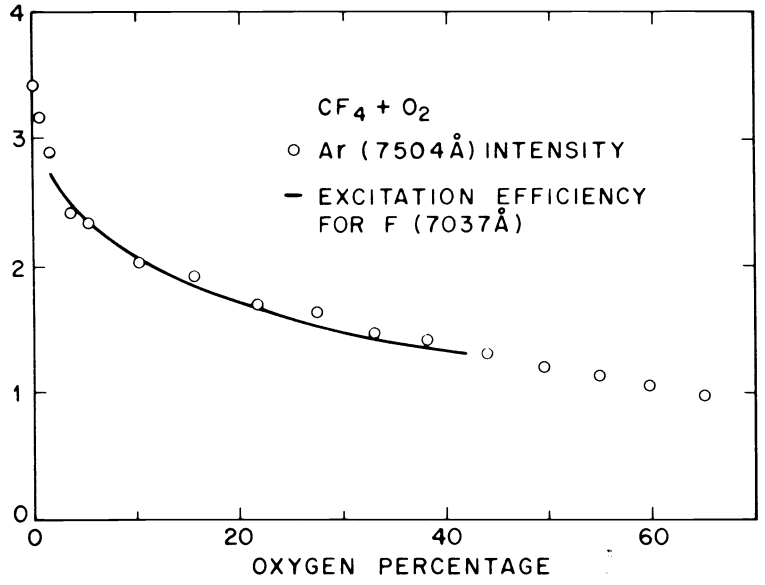

Fig. 3. Variation of α_F^e and Ar* emission intensity (at 750.3 nm) with O_2 concentration (Refs. 2 and 4).

The actinometric technique was developed independently and applied further by d'Agostino *et al.* (5-8). In studying CF_4/O_2 plasma etching of Si and SiO_2, Ar and N_2 emission were used to monitor changes in electron density as a function of O_2 concentration. Despite the difference in threshold, N_2 second positive emission (~11.3 eV) and Ar emission (~13.5 eV) exhibited the same dependence upon O_2 concentration. In addition, the intensity ratios of several F lines and of CO to CO^+ emission (covering an energy range from ≈8 to 20 eV) did not change when up to 50% O_2 was added to a CF_4 plasma. This suggests that the electron energy distribution was also invariant and that the primary

electronic change which occurs when O_2 is added to a CF_4 plasma is a decrease in charge density. This is manifest by a decrease in excitation efficiency (Fig. 3). After so characterizing the energy distribution, d'Agostino *et al.*, used N_2 and Ar emission to normalize F, O, CO, and CO_2 intensities and obtain estimates of relative changes in concentration, assuming that the emission in each case arose from electron-impact excitation of the ground-state species. Ar and N_2 were used again as actinometers in a study of SF_6/O_2 plasmas (6); but, in this case, the technique was validated *ex situ* by downstream titration measurements.

Donnelly *et al.* (9) also validated the use of Ar actinometry by downstream titration when they measured F atom concentrations in $CF_4/O_2/Ar$ and NF_3/Ar plasmas in determining the SiO_2 etching mechanism. For F atom densities from 10^{14} to 10^{16} molec cm^{-3}, Eqn. (5b) was found to hold.

In a non-intrusive *in situ* test of the actinometric technique, Ibbotson *et al.* (10) compared I^e_{Br}/I^e_{Ar} to the Br atom concentration in a Br_2/Ar plasma. The Br atom concentration was deduced from the Br_2 molecular concentration, which was measured in turn by optical absorption. This technique assumes that each dissociated Br_2 corresponds to two Br atoms. Normalized emission (I^e_{Br}/I^e_{Ar}) and concentration (N_{Br}/N_{tot}) measurements showed the same dependence on frequency over the range from 0.1 to 14 MHz. This is a noteworthy result since changes in frequency over this range can have profound effects on the electron density and energy distribution.

In studies of C_xF_y/H_2 plasmas, actinometry was pushed further when CF and CF_2 radical emission was normalized to Ar and N_2 emission (7). In this case, however, no evidence was presented to support the assumption that CF and CF_2 emission comes primarily from direct electron impact on the radical ground states. Tiller *et al.* (11) also applied actinometry to the measurement of CCl radicals produced by plasma decomposition of CCl_4 without verifying that CCl* comes from electron-impact excitation of CCl ground states.

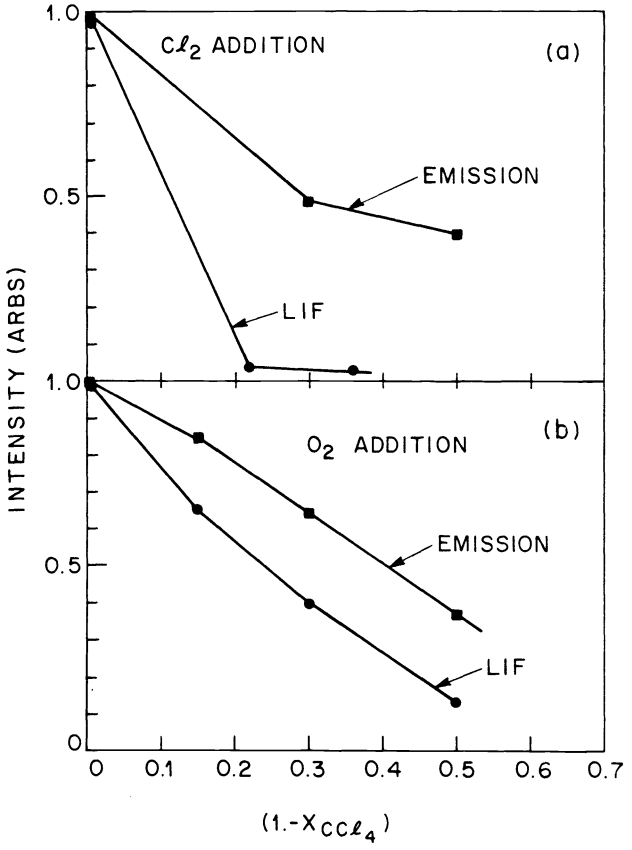

Fig. 4. CCl emission (normalized to N_2) and LIF from CCl_4 discharges as a function of Cl_2 concentration (top) and O_2 concentration (bottom) (Ref. 12).

In a non-intrusive *in situ* study, CCl radical emission was normalized to N_2 emission from $CCl_4/O_2/N_2$ and $CCl_4/Cl_2/N_2$ plasmas while the CCl radical density was measured by laser-induced fluorescence by Gottscho *et al* (12) (see Section III). As the percentage of O_2 or Cl_2 in the feedstock was increased, the CCl concentration decreased rapidly, the CCl emission decreased much less rapidly, and, N_2 emission remained constant (Fig. 4). The reason why N_2 actinometry does not work in this case is evident from LIF measurements of the CCl concentration: electron-impact excitation of ground-state CCl is relatively improbable because the steady-state concentration is low ($\sim 10^{10}$ molec cm^{-3}); the dominant mechanism for producing CCl* is electron-impact *dissociation* of CCl_x precursors. In general, actinometry is unlikely to be valid whenever the *ground-state* species is short-lived, in low abundance, and derived from a molecular parent. Thus actinometry is likely to fail for CF radicals in C_xF_y discharges but *not* for CF_2 radicals in the same discharges because CF_2 is relatively inert and long-lived (13,14).

A relatively simple way to test the validity of actinometry (non-intrusively *in situ*) is to examine emission lineshapes. Because electronic to translational energy transfer is inefficient, line-widths generated by electron-impact excitation are generally narrower than line-widths resulting from electron-impact dissociation. Since dissociation ordinarily occurs by excitation to a repulsive electronic state, fragment radicals often leave with excess translational energy (15). Using a Fabry-Perot interferometer, Gottscho and Donnelly (16) found that the F* translational energy distribution in a $CF_4/O_2/Ar$ plasma was generally cold like that for Ar*. Over a range from 0 to 50% O_2 in CF_4 (with 5% Ar), the F* and Ar* temperatures remained constant and equal to 360 ± 70K. These observations suggest that F* is formed primarily by electron-impact on F ground-state and should quell the lingering doubts about the validity of actinometry in the $CF_4/O_2/Ar$ system.

In Cl_2/Ar plasmas, on the other hand, the Cl* and Ar* translational temperatures were equal and cold only in the plasma center. In the sheath, the Cl* emission lineshape was distinctly non-Gaussian, with a broad pedestal superimposed on a sharp, central peak. The relative intensity of the broad pedestal increased on the negative part of the cycle in these low frequency (20-100 kHz) plasmas, suggesting that an ion-molecule reaction produces some Cl*. Ar* also showed a pedestal during the negative part of the cycle (Fig. 5). These observations are consistent with the results of Flamm and Donnelly (17), who showed that time-dependent Cl* and Ar* emission (at 250 kHz) have the same functionality in the plasma center but not in the plasma sheaths. In this case, it is concluded that Ar cannot be used as an actinometer for determining N_{Cl} in the electrode sheaths.

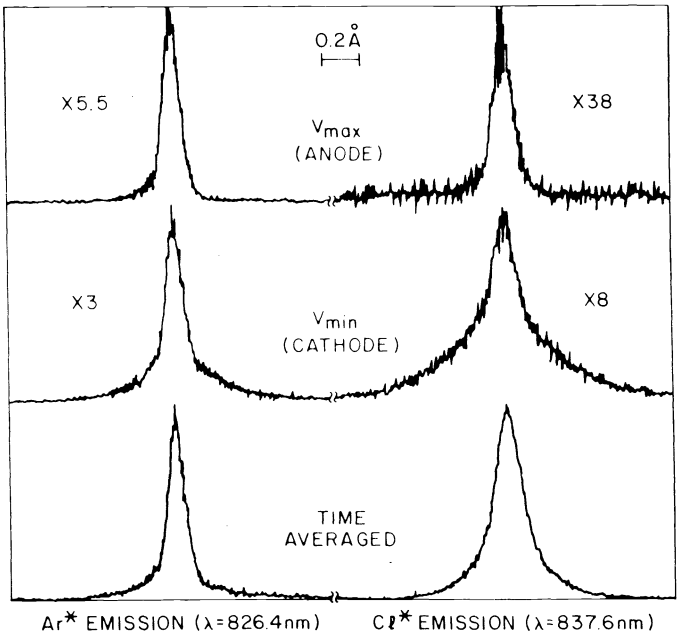

Fig. 5. Ar* (left) and Cl* (right) emission lineshapes as a function of time during the (50 kHz) rf cycle 1 mm above the powered electrode: at the voltage maximum (momentary anode), top; at the voltage minimum (momentary cathode), middle; and time-averaged (bottom) (Ref. 16).

C. Temperature Measurements

Spectrally resolved electron-impact emission can be used to determine rotational and vibrational temperatures providing the emission is short-lived and results primarily from direct excitation of ground-state species (18). If chemiluminescence or electron-impact induced dissociation are sources for emission intensity or the excited-state collisionally relaxes on a time-scale which is fast compared to its emission rate, the temperatures obtained will be valid for only the excited state. We will mention only a few recent studies relevant to plasma processing. Of course, it must always be remembered that the glow discharge is a non-equilibrium system and a single temperature is almost never adequate to describe the energy distributions for all degrees of freedom of all atoms and molecules.

As a measure of carrier gas temperatures, optical emission from inert molecules such as N_2 and CO is probably reliable. Harshbarger and Porter (19) showed recently that N_2 second positive emission ($C^3\Pi_u \rightarrow B^3\Pi_g$) from a N_2 discharge can be accounted for by direct electron-impact excitation of $X^1\Sigma_g^+(v''=0)$: the vibrational intensity distribution is a convolution of the $C^3\Pi_u \leftarrow X^1\Sigma_g^+$ $(v''=0)$ excitation and $C^3\Pi_u \rightarrow B^3\Pi_g$ emission Franck-Condon factors. These same authors had used N_2 emission previously (20) to measure a rotational temperature of 595 ± 30K in an rf (13.56 MHz) discharge through N_2. Oshima (21) determined rotational temperatures from CO emission, formed in C_2F_6/O_2 plasmas. He reports values for T_r which range from 400 to 600K depending upon gas composition and applied power. DeBenedictis *et al.* found similar results from CO emission excited in CO/He plasmas (22). Although these authors report substantial vibrational excitation of CO, they apparently deconvolved the observed vibrational band intensities with respect to only the emission and not the excitation Franck-Condon factors.

Davis and Gottscho (23) verified the use of optical emission from N_2 and N_2^+ in determining T_r by comparing optical emission measurements to laser-induced fluorescence (LIF) measurements (Section III). In N_2 discharges, the two techniques gave consistent values for T_r, demonstrating that emission line intensities can be used for ground-state rotational energy distribution measurements. In CCl_4/N_2 mixtures, T_r values from radical CCl LIF and N_2^* were generally consistent except near cooled electrodes where the CCl temperatures were slightly colder, probably as a result of ion sputtering of cold adsorbates.

Optical emission may also be useful as a measure of the electron temperature. Again, the same constraints mentioned above apply here. D'Agostino *et al.* (5) examined the intensity ratios of lines with different energy thresholds to deduce that changes in the electron temperature were negligible as CF_4 was diluted with O_2. In a similar fashion, Mehs and Niemczyk (24) used various Ar and Fe lines to deduce electron temperatures of ≈2000-5000K in a hollow cathode discharge.

D. Time-Resolved Emission

Recently, emission from rf discharges has been time-resolved in order to obtain dynamical information on the excitation function (17,25,26). These studies are similar to those on ionization waves in dc discharges, for which a more extensive review can be found elsewhere (27). The primary difference is that while ionization waves in dc discharges stem from slowly evolving instabilities, in rf discharges they are driven by high frequency applied fields. The experimental configuration used for time resolution is like that for any optical emission experiment except that the photomultiplier tube output is fed into a gated integrator which is triggered, in turn, by a reference waveform locked to the applied voltage (Fig. 6).

In low frequency (250 kHz) Cl_2/Ar plasmas, Flamm and Donnelly (17) found that the optical emission from Cl^*, Cl^{+*}, Cl_2^{+*}, and Ar^* were in phase with the voltage waveform in the momentary positive (anode) electrode sheath but lagged the voltage in the momentary negative (cathode) electrode sheath. The delay was attributed to the sheath transit time for ions, which eject secondary electrons upon electrode impact. The secondaries then excite emission as they traverse the sheath. Gottscho *et al.* (26) made similar observations in N_2 plasmas (at 20-90 kHz) except that no phase delay was apparent during the negative cycle; this difference may be a result of the greater mobility of N_2^+ (or N^+) ions in N_2 compared to Cl_2^+ (or Cl^+) in Cl_2 and Ar as well as the lower frequency range employed in the latter experiment. Flamm and Donnelly (17) also noted that the emission was 100% modulated throughout the discharge because the electron energy distribution relaxes on a time-scale which is fast compared to one-quarter period of the applied potential (28).

At higher frequencies (>1 MHz), larger phase shifts and smaller modulation are observed (17,25). The phase shift was found to be dependent upon position from the electrode surfaces: the excitation wave propagates away from the cathode and narrows to a pulse with FWHM of ~10 nsec, much shorter than the applied voltage period (74 nsec for 13.5 MHz) (25). An explanation for the formation of this pulse is still wanting.

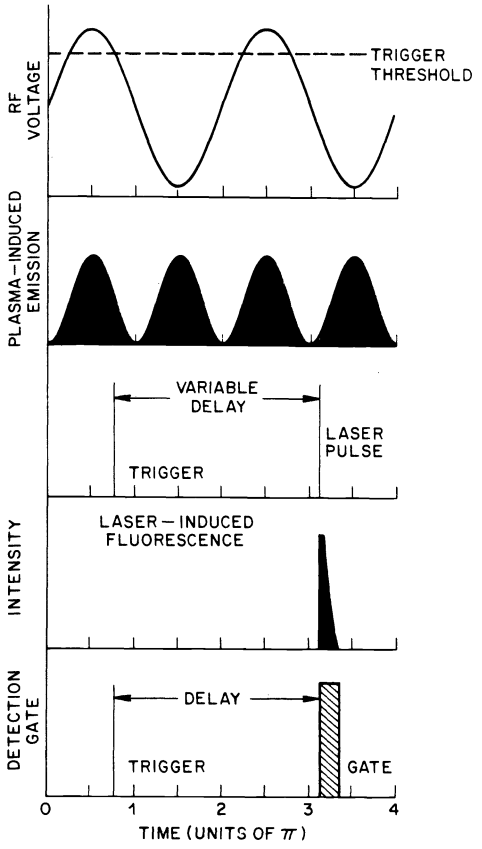

Fig. 6.

Schematic timing diagram illustrating manner by which time-resolved optical emission and LIF are recorded (Ref. 26).

In general, we have seen that optical emission is most useful for qualitative analysis and semi-quantitative characterization of energy distributions and excitation phenomena. In some instances, actinometry can be used to improve its quantitative utility.

III. LASER-INDUCED FLUORESCENCE

From the above discussion it is clear that emission spectroscopy has a useful role to play in plasma diagnostics but that there are also very definite limitations upon the technique. Most particularly one desires non-intrusive optical techniques which monitor directly the ground (or metastable) state populations of the active species. In principle laser induced fluorescence (LIF) is precisely such a technique. Fig. 7 shows a schematic diagram of an experimental LIF apparatus. One passes a tunable

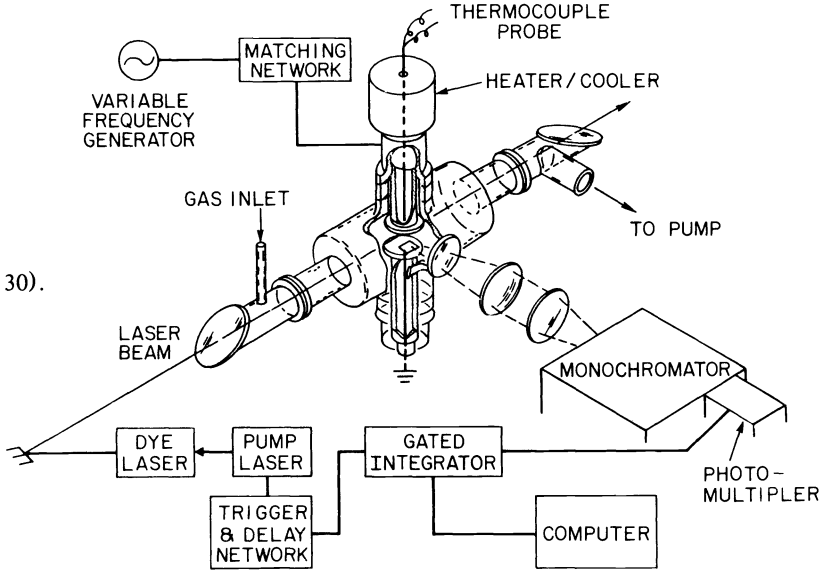

Fig. 7.

LIF schematic (Ref. 30).

dye laser through the plasma and collects laser induced fluorescence perpendicular to the laser axis. Typically one uses a pulsed dye laser and a gated detection system to reject the continuous background emission from the discharge. An excitation spectrum of the species of interest is recorded by sweeping the laser frequency and monitoring the intensity of laser induced fluorescence. Typically for plasma experiments the fluorescence is dispersed through a monochromator which serves as both a spatial and spectral filter to discriminate against the plasma background. When an excitation spectrum is recorded a relatively wide monochromator bandpass is employed; alternatively the laser frequency can be fixed on an excitation spectrum feature and the monochromator scanned with a narrow bandpass to record a laser-excited, wavelength-resolved emission spectrum. By employing such techniques the species monitored can be unambiguously identified.

For such an experimental set-up the laser induced emission, I_r^ℓ, of a reactive species can be related to its concentration [r] by an equation of the form (Eq. 2b), that we used to describe emission, i.e.

$$I_r^\ell = \alpha_r^\ell [r] \tag{6}$$

and in analogy with Eq. 3

$$\alpha_r^\ell = K \int_0^\infty Q(P, N_e)\, \sigma_r^\ell(\epsilon)\, N_\ell(\epsilon)\, d\epsilon \tag{7}$$

$\sigma_r^\ell(\epsilon)$ = cross-section for laser excitation of the ground state species r.

$N_\ell(\epsilon)$ = number of laser photons available at energy ϵ.

The quantum yield function $Q(P, N_e)$ is exactly the same as before.

At first glance it may appear that we have gained nothing by replacing Eqs. 2 and 3 respectively by 6 and 7. However under most conditions Eq. (7) for α_r^ℓ greatly simplifies. The cross-section $\sigma_r^\ell(\epsilon)$ is discontinuous as a function of ϵ, thereby defining the line nature of the LIF excitation spectrum. Since we can externally control the number of laser photons and their frequency, i.e. ϵ, we can choose to evaluate α_r^ℓ at the maximum of a particular line, i, in the spectrum. In that case

$$I_r^\ell = \alpha_r^\ell [r] = K\, Q(P, N_e)\, F_{ri}\, N_\ell [r]$$

$$\approx K\, F_{ri}\, N_\ell [r] \tag{8}$$

where in the last equality $Q(P, N_e)$ is assumed unity and F_{ri} is the maximum oscillator strength for a particular transition i of species r. In principle the quantity F_{ri} is directly calculable (23,29,30) and K is determinable by calibration of the detector. Thus one has a direct measure of the concentration [r] of the ground state species r, essentially independent of discharge conditions, gas mixture, etc.

Eq. 8 is applicable for the volume of the reactor intersected by the laser and the field of view of the detector. Such a volume can be made quite small, e.g. $\lesssim 1$ mm^3, thus one can probe different spatial regions of the reactor. In a similar manner the laser pulse is very short ($\leqslant 10$ nsecs), so the time resolution of the technique is very high. The overall sensitivity of the LIF technique is also very high. Numerical evaluation of the quantities appearing in Eq. 8 leads to detectable signals for [r] as low as 10^6/cm^3 and less.

It should be pointed out that the concentration [r] given in Eq. 8 is the concentration of the particular quantum state in which the transition originates. If the molecular internal states are thermally equilibrated and their temperature known, the concentration [r] may be related to the species concentration in all levels using the well-known Boltzmann relation (23,30). By changing the dye laser frequency, the relative populations of many quantum states can be measured. From this information, the extent of thermal equilibrium can be established and the temperature of the species determined.

It is usual for the translational and rotational degrees of freedom to be equilibrated for a given species in a plasma. However, the degree of equilibration between ions and neutrals is still open to questions. LIF is an excellent tool for measuring the internal rotational temperatures of the various species directly in their ground states. As discussed above (Sec. II.C), emission spectroscopy provides similar information for the excited states.

A. Concentration Measurements: Radicals

There are several reasons for wanting to know the concentrations of various radicals produced in rf plasmas. The most obvious reason is to be able to control the heterogeneous chemistry by changing the plasma composition and radical transport to device surfaces. Small radicals are suitable for measurement by LIF in that Q is often nearly unity. To date, the most extensive LIF studies of radicals

in plasmas have been for CF_2 and CCl radicals in fluorocarbon (31,32) and chlorocarbon (12) discharges, respectively.

Hargis and Kushner (31) measured relative CF_2 concentrations by LIF with a KrF excimer laser (248 nm). Since a fixed frequency laser was used, no knowledge of the internal energy distributions was obtained but it is likely that the levels sampled were representative of the total CF_2 concentration, which was examined as a function of applied power (at 13.56 MHz). C_2F_6 plasmas were found to generate about four times as much CF_2 as CF_4 plasmas. In both systems, the CF_2 density increased super-linearly with rf power.

In a separate LIF study, Pang and Brueck (32) measured CF_2 concentrations in $CF_4/O_2/H_2$ plasmas with a quadrupled Nd:YAG (266 nm) laser. Again, the internal energy distribution was not characterized. They found a similar dependence of $[CF_2]$ on rf power to that obtained by Hargis and Kushner (31). In addition, they examined the dependence of $[CF_2]$ on pressure, frequency, O_2 concentration, and H_2 concentration. As expected, $[CF_2]$ decreased as O_2 was added to the feedstock because of oxidation reactions which form CO and CO_2 and liberate free fluorine (33,34). Also as expected, H_2 addition caused $[CF_2]$ to increase because of abstraction reactions which result in HF formation (35). As the frequency was increased from 4 to 14 MHz, $[CF_2]$ was found to increase markedly most likely because of increased charge density at higher frequency (30).

Gottscho *et al.* (12) used a tunable dye laser to monitor relative changes in CCl radical density by LIF as a function of power, flow-rate, pressure, electrode temperature, feedstock composition, and position between the electrodes. Because of the dye laser's tunability, it was possible to select rotational transitions in the $A^2\Delta - X^2\Pi$ band system which are temperature insensitive and therefore truly representative of the total CCl concentration. The spatial variations in concentration as a function of pressure show clearly that CCl* emission is a poor measure of [CCl] (Fig. 8). At low pressure (155 m Torr = 20.6 Pa) (Figs. 8a and 8b), where the mean lifetime for ground-state CCl is comparable to or longer than the diffusion time, the [CCl] spatial profile is dictated primarily by the thermal gradient imposed across the gap (12): the left electrode was heated to 300°C while the right electrode was water-cooled. By contrast, CCl* emission exhibits maxima in both electrode sheaths and is relatively insensitive to thermal gradients. At higher pressure (106 Pa, Figs. 8c and 8d), both CCl concentration and emission profiles show strong maxima in the electrode sheaths and only weak signal strengths in the plasma center. These changes as a function of pressure are readily understood when one considers the differences in lifetime for the excited $A^2\Delta$ and ground $X^2\Pi$ states of CCl. The $A^2\Delta$ state has a radiative lifetime of 105 ± 3 nsec and a quantum yield which changes from ≈90% to ≈60% when the pressure changes from 20.6 to 106 Pa (36). Because the $X^2\Pi$ density is low ($\lesssim 10^{10}$ molec cm^{-3}) and the $A^2\Delta$

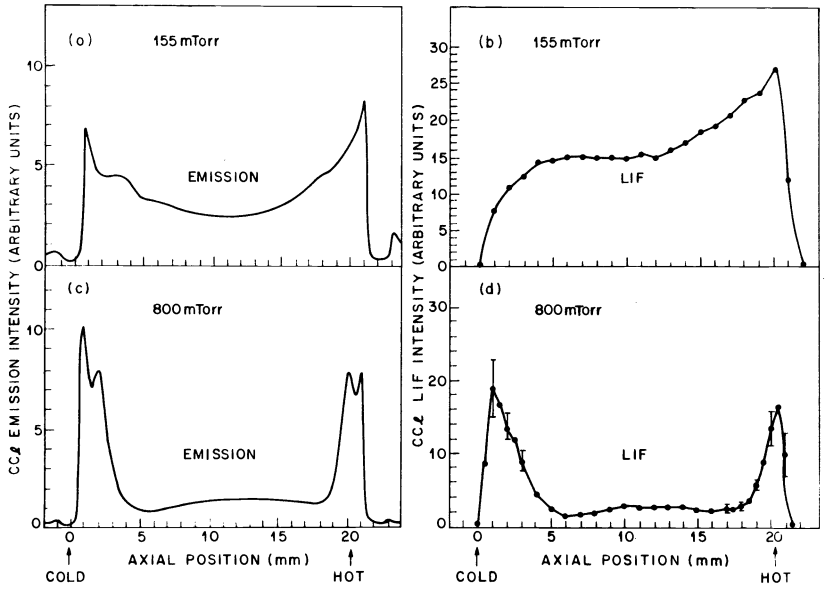

Fig. 8. CCl emission (left) and LIF (right) vs. position for two different pressures in a CCl_4 discharge: top, 20.6 Pa (0.155 Torr); bottom, 106 Pa (0.800 Torr). The electrode on the left is heated to 300°C while the right electrode is water cooled.

lifetime is short, CCl* emission arises mainly from electron-impact dissociation of CCl_x species and is mostly a measure of the overall rate of CCl formation. The $X^2\Pi$ state, on the other hand, has a lifetime of $\approx$50 μsec at 1 Torr (12,14), which is most likely governed by reactive collisions such as $CCl + CCl_4 \rightarrow CCl_2 + CCl_3$. At higher pressure, the $X^2\Pi$ state cannot diffuse far from its site of formation without being lost by reaction. Thus, the emission and concentration profiles are similar at higher pressure since both reflect the CCl formation rate.

The observation that CCl radicals are formed in the electrode sheaths is consistent with a model for CCl_4 decomposition by dissociative electron attachment (12). The CCl_4 electron attachment cross section is strongly peaked only at energies below 10 eV, with the largest peak at $\approx$0 eV. Slow electrons are readily captured by CCl_4 (and presumably by CCl_x species as well) to form metastable negative ions (e.g. CCl_4^-) which subsequently dissociate and produce radicals such as CCl_3 or CCl and stable negative ions such as Cl^- (37-40). The slowest electrons in the plasma can be found close to the electrodes because this is where the potential is most negative: secondary electrons formed by either ionizing collisions or ion-impact of the electrodes have not yet undergone acceleration by the field; similarly, plasma electrons have been slowed by the large negative sheath potential. The end result is that radicals such as CCl are formed predominantly in the sheath but will be confined there only when the reactive loss rate exceeds the diffusion rate.

In another application of LIF to plasma diagnosis, Uchino *et al.* (41) monitored the n=2 and n=3 levels of hydrogen by exciting the Balmer alpha transition and detecting plasma-induced emission, respectively. They used these measurements to deduce the amplitude of ion-acoustic turbulence across a potential step in a low pressure dc discharge through H_2. This experiment is noteworthy for two reasons: (i) it illustrates that LIF can be used to measure highly excited but metastable level populations of atomic radicals and (ii) that LIF can be detected sensitively in the presence of not only intense plasma-induced emission but also intense laser radiation of the same wavelength.

B. Concentration Measurements: Ions

Donnelly *et al.* (30) looked at the time-averaged concentration of Cl_2^+ ions in a Cl_2 plasma as a function of frequency, power, pressure, feedstock composition, and distance from the electrodes. The dependence of $[Cl_2^+]$ on frequency was of primary interest, since frequency can play an important role in etching and deposition (30,42,43). As frequency was varied from 13 MHz to 0.01 MHz, a minimum in the Cl_2^+ density, most pronounced in the sheath at low power density, was observed at $\approx$1 MHz (Fig. 9). This frequency roughly corresponds to the ion plasma frequency, above which the ions can no longer respond to the applied rf potential. At low frequencies, (<1 MHz) ions can follow the field (26,43) and impact electrode surfaces with sufficient energy to generate secondary electrons, which are then accelerated and produce ionization as they cross the sheath. As the ion plasma frequency is approached, however, the sheath field decreases, ion-impact no longer produces many secondary electrons, and the charge density decreases. Above 1 MHz, the charge density begins to increase again, but the mechanism by which this occurs is not well understood.

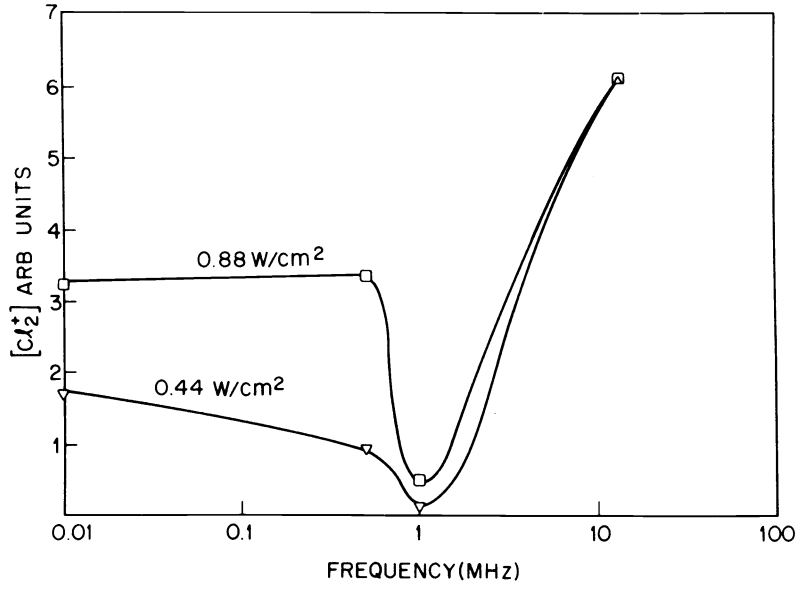

Fig. 9. Cl_2^+ (LIF) vs. freq. (Ref. 30).

In order to monitor the dynamics of low frequency plasmas, Gottscho *et al.* (26) measured N_2^+ and Cl_2^+ ion densities by time-resolved LIF. In these experiments, the dye laser used to probe ground state populations is pulsed synchronously with the applied rf potential in order to sample the instantaneous ion concentrations anywhere in the gap (Fig. 6). In the plasma center, the N_2^+ and Cl_2^+ populations were found to be only weakly modulated when pure N_2 and Cl_2 plasmas were examined. The extent of modulation was used to estimate 1st order ground-state lifetimes as a function of pressure for N_2^+ and Cl_2^+: at 0.3 Torr, 30-35 μsec for both ions. These times probably represent loss by ambipolar diffusion. When 10% Cl_2 was added to the N_2 plasma, the N_2^+ lifetime decreased to 1.5 μsec while the Cl_2^+ lifetime increased. This indicates that the charge exchange reaction $N_2^+ + Cl_2 \rightarrow Cl_2^+ + N_2$ occurs readily in N_2/Cl_2 plasma mixtures ($k \sim 6 \times 10^6 sec^{-1} Torr^{-1}$).

In the electrode sheaths, the ionic response to the applied potential was characterized in terms of an oscillating sheath front. At any position in the sheath, the ion population first grows because of electron-impact ionization of neutral N_2 or Cl_2; but, as the sheath front propagates out from the electrode surface, ions are rapidly accelerated toward the surface while electrons are repelled toward the plasma center (Fig. 10). Over the frequency range studied (20-90 kHz), the sheath propagation velocity (determined from the line in Fig. 10) was found to increase linearly with frequency so that the sheath front reached the distance of maximum sheath expansion, d, in one-half period; over the same frequency domain, d was observed to be a function of pressure and gas composition only. For N_2 plasmas and lower pressures, d was larger than for Cl_2 plasmas and higher pressure. The pressure dependence was also observed by Donnelly *et al.* (30) in their time-averaged LIF experiments and is consistent with reduced charge mobility and increased charge density at higher pressures. Cl_2 plasmas exhibit smaller sheaths for similar reasons: the higher electronegativity for Cl_2 reduces negative charge mobility and the lower ionization potential for Cl_2 leads to higher charge densities.

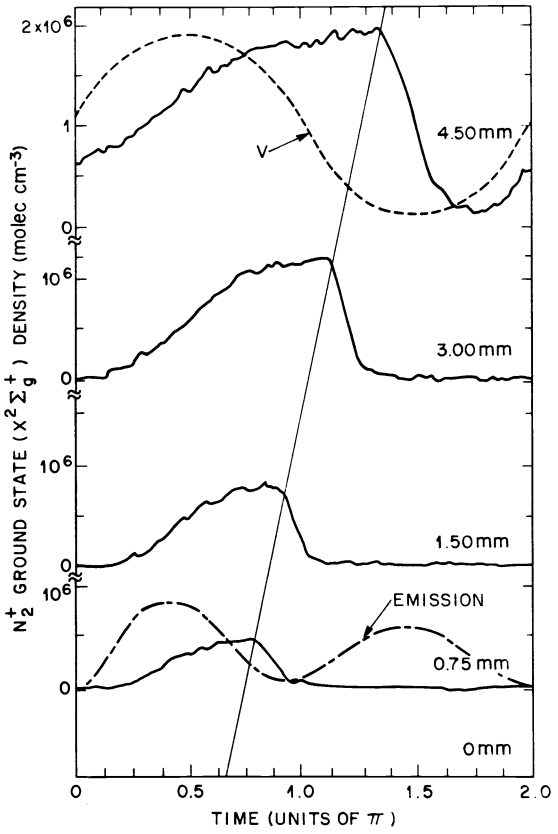

Fig. 10.

N_2^+ LIF conc. vs. time during the rf cycle for four positions in the sheath. For comparison the applied voltage waveform is shown at the top and plasma-induced emission is shown for a position 0.75 mm from the electrode at the bottom.

C. Energy Distribution Measurements

Because of the tunability and resolution of LIF, it is nearly ideal for measuring internal energy distributions of ions and radicals in rf plasmas (23,30,44). Most measurements have been made on the rotational energy distributions and in every case reported so far, the distributions could be represented by a single rotational temperature, T_r. Donnelly *et al.* (30) saw little dependence of the Cl_2^+ rotational temperature on distance from the water-cooled electrodes or on applied frequency (0.25 or 13 MHz);

they measured an average T_r of 350K. Davis and Gottscho (23) investigated the influence of surface temperature and rf power on the CCl rotational temperature profile across the electrode gap in a CCl_4 plasma at low frequency (55 kHz). They found little dependence of T_r on position except near the electrodes, where gradients as large as 10^2K mm^{-1} were observed. The dimensions of the thermal gradient are consistent with known mean free paths for rotational relaxation; the magnitude of the gradient and the temperature in the plasma center are governed by both electrode temperature and rf power density.

No detailed LIF studies of vibrational energy distributions in plasmas have yet been reported, although hot bands have been excited in CCl (23) and N_2^+ (26). The results obtained suggest that the vibrational "temperature" is substantially greater than the rotational temperature as is expected from their different rates of relaxation.

Nor have detailed LIF studies of translational energy distributions been reported yet. There are two reasons for this: (i) for radicals (or ions in the discharge center), a narrow frequency, cw laser would be required to accurately measure Doppler line shapes at temperatures less than 1000K but all LIF studies of plasmas to date have utilized pulsed lasers with linewidths comparable to or greater than the Doppler width; and (ii) for ions, the broader energy distributions expected to occur in the sheath (45), have not been observed by LIF because the steady-state ion concentrations are so low ($\lesssim 10^6$ molec cm^{-3}) as a result of acceleration by the sheath field (26,44). While the first limitation can be circumvented, the second limitation is more fundamental. Measurements of the ion translational distribution in the sheath require techniques other than LIF, such as laser optogalvanic spectroscopy (LOG) (44). It should be mentioned that a high resolution cw laser has been used to measure the absorption line strength and shape of OH in an H_2O discharge, which give both T_r and T_t (46).

IV. OTHER TECHNIQUES

A. Opto-Galvanic Techniques

A diagnostic technique very closely related to LIF is laser optogalvanic spectroscopy (LOG). The effect was first discovered in discharges over 50 years ago, with an atomic lamp standing in for the laser. However, the development of tunable lasers has greatly widened (47) the applicability of the technique.

A schematic diagram of a typical LOG apparatus is shown in Fig. 11. Just as in LIF, an excitation spectrum of a species of interest is obtained by scanning a tunable dye laser through one of the species' electronic absorptions. However rather than detecting fluorescence created by the absorption of laser photons, optogalvanic signals result from changes in the impedance of the discharge in response to the absorption of laser radiation. Usually the impedence change is monitored as a change in voltage across a DC discharge as shown in Fig. 11. For rf discharges, laser induced impedence changes are detected either by monitoring the response of the driving circuit or by a separate RF antenna.

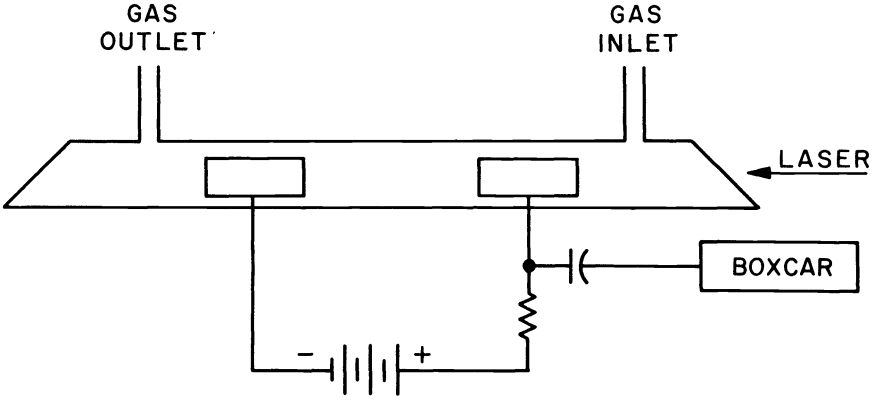

Fig. 11. LOG apparatus.

The spectra of numerous atomic species, ions, free radicals, and relatively unreactive feed gases, have been obtained in discharges by the LOG technique. The chief disadvantage of the LOG experiment as a plasma diagnostic is in the relation of the observed LOG signal strength to the concentration of the carrier species. If one writes an equation of the form of 2 or 6 then the functional form of the proportionality factor α is not even clear. In simplest terms the absorption of a laser photon with the concommitant change of electronic state in the absorbing species causes the observed impedence change in the discharge. However the detailed relationship between photon absorption and impedance change is generally very complex.

A typical mechanism would be the production of an excited state of a neutral atom or free radical; this excited state could be more easily ionized leading to more ions, more discharge current, and less apparent discharge impedance. Conversely the laser excitation could lead to a less easily ionized state, giving fewer ions and thus a higher impedence. Indeed signals of opposite polarity are often observed in LOG spectra and a given transition can change polarity as a function of discharge current or pressure. Usually there are many competing processes in the plasma and the absorption of laser photons simply shifts the balance.

As the above discussion implies LOG is likely an unreliable tool for quantitative determination of species concentrations. However it may still be quite useful as a plasma diagnostic because the very processes — ionization, electron attachment, photodetachment, and recombination, which are responsible for the generation of LOG signals — are the same processes that sustain and control the discharge. By studying the LOG signals in concert with other information, say LIF signals from the same species, it may be possible to unravel the complex kinetics governing the plasma.

Another instance of the usefulness of LOG spectroscopy is the situation where other spectral signatures of a species are absent but LOG signals are present. An important example of such a situation is the cathode sheath region of an rf discharge. As pointed out earlier LIF detection of N_2^+ is easily seen in the center of such a discharge but is not detectable in the cathode sheath because the higher ion velocities there limit its concentration. Walkup, Dreyfus, and Avouris (44) have recently reported LOG signals for N_2^+ in the sheath region of the discharge, while the LOG signal drops below detectability in the center of the discharge. It is argued that the high sensitivity for LOG detection of N_2^+ in the sheath results from an effective increase in ion mobility due to a smaller cross section for charge exchange collisions in the excited state.

The obtainment of the LOG signal of N_2^+ in the sheath allows a measurement of its rotational temperature which is warmer than in the rest of the plasma. Also Doppler broadening was detected for N_2^+ moving along the electric field lines (44).

B. Infrared Techniques

Surprisingly few applications of infrared spectroscopy to plasma processing have been reported. Fourier transform infrared (FTIR) emission spectroscopy has been used in characterizing low pressure silane (48) and air (49) plasmas but IR emission is subject to the same limitations as optical emission and is useful mostly for qualitative analysis. Knights *et al.* (48), using a globar source and FTIR, measured the spectra of SiH_4 and SiH in rf (27.3 MHz) plasmas. They made no attempt to obtain spatial information and were unable to detect polyatomic radicals, such as SiH_2 and SiH_3. From rovibrational line intensities, they determined the following vibrational and rotational temperatures: for SiH_4, T_v=850K and T_r=300K; for SiH, T_v=2000K and T_r=484K. The non-equilibrium between vibration and rotation is consistent with LIF experiments and is not surprising since vibrational relaxation generally proceeds more slowly than rotational relaxation. Nor is it surprising that the SiH_4 parent is cooler than the SiH radical, which is formed predominantly by electron-impact dissociation. In another IR absorption experiment the decomposition of CF_4 and C_2F_4 was investigated (50).

Based on recent experiments, we expect that infrared laser techniques will make a significant contribution to plasma diagnosis. Hirota *et al.* (51-53) have used tunable diode laser spectroscopy (TDLS) to record the absorption of several free radicals (e.g. CCl, NS, and CS) created in ac plasmas. The concentrations of these species were not measured, but they are likely to be as low as 10^9-10^{10} molec cm^{-3} (12). Very recently, DeJoseph *et al.* (54) used TDLS to measure SiH_4 concentrations ($\sim 10^{12}$-10^{14} molec cm^{-3}) downstream from a dc discharge (i.e. *ex situ*). Fluorine (55) and chlorine (56) atoms have also been detected by TDLS but, again, only in *ex situ* experiments. Stanton and Kolb (55) demonstrated a detection sensitivity for the electric-dipole forbidden transition $^2P_{3/2} \rightarrow {}^2P_{1/2}$ in F of $\sim 10^{15}$ atoms cm^{-3} and suggested that this could be lowered to $\sim 10^{12}$ atoms cm^{-3} by using multi-pass optics and derivative detection.

Oka *et al.* (57) used TDLS *in situ* to measure Doppler shifts for different rotational and vibrational levels of ArH^+ ions created in a dc glow discharge (Fig. 12). From these shifts, drift velocities were determined, which in conjunction with probe measurements of the axial electric field, provided an estimate of the ionic mobility. A similar type of measurement was made by Saykally *et al.* (58,59) using a color center laser to detect HCO^+ and HNN^+ ions, whose motion was modulated by a low frequency (1-8 kHz) driving potential. In these experiments, the primary emphasis was on the rotation-vibration line positions; the ion drift velocity was used to enhance the detection sensitivity with respect to unaccelerated neutrals.

In another IR laser experiment, Farrow and Richton (60) used a CO_2 laser to monitor the rotational temperature (675 ± 75K) and degree of dissociation (5-20%) of BCl_3 in an rf (13 MHz) discharge.

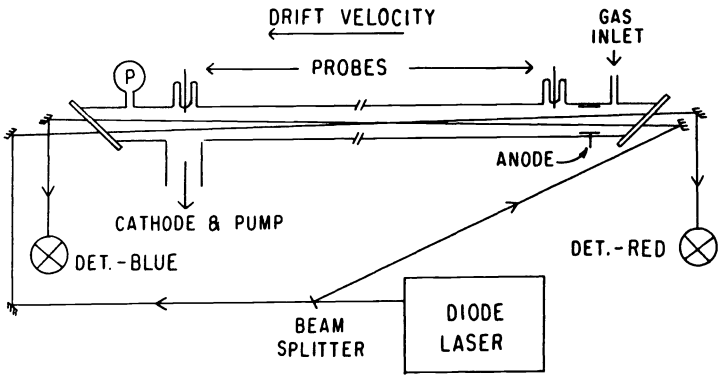

Fig. 12. Diode laser apparatus (see Ref. 57).

All of these experiments clearly demonstrate the capability of IR techniques for *in situ* monitoring of the concentrations and energy distributions of radicals, ions, and parent gases found in low pressure plasmas. Although spatial information has not been obtained yet, there is no reason why tomographic techniques could not be employed to circumvent the line-of-sight limitations of absorption spectroscopy (61,62). Application of TDLS to plasma processing seems particularly promising because of the compactness and relative economy of diode laser sources.

C. Raman Techniques

Raman spectroscopy has yet to be exploited as a plasma diagnostic tool despite its inherently high spatial resolution and ubiquitous use elsewhere. Like LIF, both spontaneous and coherent Raman techniques entail detection of scattered photons; but, unlike LIF, Raman scattering does not rely upon creation of a fluorescent excited state and is not sensitive, therefore, to excited state quenching.

Several recent applications of Raman scattering to detection of atomic radicals are encouraging (63-67). Cummings and Aeschliman (63) measured the spontaneous Raman scattering cross section for the $^2P_{3/2} \rightarrow {}^2P_{1/2}$ fine-structure transition in fluorine. They used a cw Ar^+ laser at 488 nm (1.1 W), focussed into a heated monel cell containing an equilibrium mixture of F and F_2. The rotational Raman signal from F_2 was used to determine the temperature, which in turn was used to determine the F atom density ($\sim 10^{15}$-10^{17} atoms cm^{-3} for T=600 to 850 K). In an *ex situ* experiment, Moore (64) utilized coherent anti-Stokes Raman scattering (CARS) (see Ref. 65) to detect the corresponding fine-structure transition in Cl, formed upstream in a microwave discharge. In this experiment a Nd:YAG laser was used as a pump for both the CARS signal and for a dye laser whose output is used as the tunable Stokes frequency (65). Moore also detected nonresonant CARS from Cl_2 but saw no change when the discharge was switched on or off. The Cl atom density was measured by titration with NO or Br_2 using the disappearance of the CARS signal as an end point indicator. A detection limit of $(4.5 \pm 1.7) \times 10^{15}$ atoms cm^{-3} was reported but this might be improved by two orders of magnitude by using narrower bandwidth lasers (64). Very recently, CARS has been used to measure the degree of SiH_4 decomposition in a DC glow discharge at $\approx$0.5 Torr as a function of position between the electrodes and as a function of pressure (67).

Hargis (68) has shown that the sensitivity of spontaneous Raman scattering can be made comparable to that for coherent Raman techniques by simply using an UV source. He demonstrated this by using a KrF excimer laser (248 nm) to induce Raman scattering from N_2 at partial pressures as low as 10^{-4} Torr.

Certainly, the primary reason why Raman spectroscopy has yet to be used extensively as a low pressure plasma diagnostic is its lack of sensitivity. However, we anticipate that Raman techniques will prove useful in measuring the degree of dissociation and temperature (69) of both feedstock constituents and abundant ($\gtrsim 10^{14}$ atoms cm^{-3}) radical atoms.

D. Multiphoton Techniques

It is appropriate to return to the species, with which we began our discussion, the light atoms, F and O. Fig. 13 shows a generic energy level diagram appropriate to all the reactive light atoms in the first two or three rows of the periodic table. The key feature of this diagram is the very large gap in energy between the ground and first excited state, followed by a large number of levels between the first excited state and the ionization limit. It is between these latter states that the transitions occur which were used for the emission diagnostic of the CF_4-O_2 plasma.

In our discussion of that work we pointed out both the importance of the emission diagnostic for

understanding the CF_4-O_2 plasma and the limitation in the technique, which centered around the uncertainities in α^e the proportionality "constant" between concentrations and emission intensities and the mode of production of the excited state. Because of these uncertainities and the importance of light atoms for plasma processes, it may seem strange that a more "quantitative" diagnostic, like LIF, has not been applied to light atom detection. Fig. 13 gives the obvious answer, all transitions in such atoms

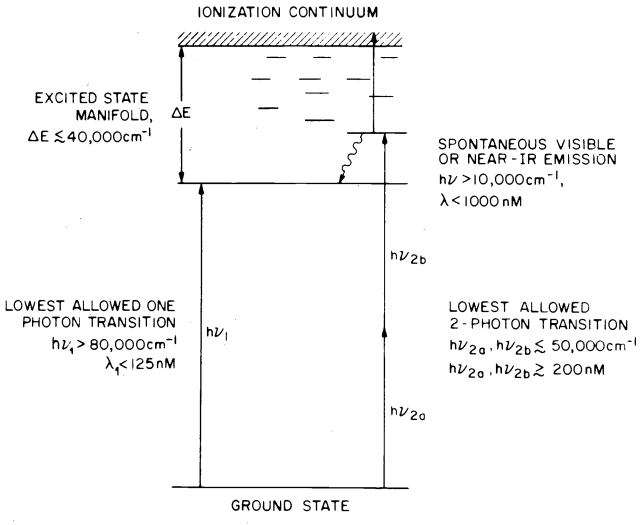

Fig. 13. Schematic energy level diagram for "light" atoms. On the left hand side a one-photon transition is illustrated, on the right a two-photon transition. This energy level diagram applies to H, N, O, C, F, Cl, Br and other "light" atoms. The only exception to the stated energy intervals is for F atoms (Ref. 74).

from the ground state lie in the extreme UV spectral region, well beyond the reach of today's tunable lasers. The key to the solution of this problem, as shown on the far right of Fig. 13, is the use of two photons, rather than one, to reach one of the lower excited states. The requirement on the laser wavelength is then typically shifted into the 200-300 nm range, a difficult but not impossible region for the generation of intense, tunable laser outputs.

This 2-photon LIF has presently been successfully applied to the detection of the light atoms, H (70), N (71), O (72,73), S (74) and Cl (74). These experiments bring all the traditional advantages of LIF probes, high temporal and spatial resolution coupled with reliable relations between signals and concentrations, to the detection of the light atoms. So far the successful experiments have been *ex situ* in nature, i.e. the 2-photon LIF of the atoms was accomplished downstream of the discharge source. Experiments are presently underway aiming towards *in situ* 2-photon detection and monitoring of these same atoms.

V. CONCLUSION

It should be clear by now that no single diagnostic technique is adequate to characterize plasma chemistry or to provide process control. Optical emission is primarily useful for characterizing the electron energy distribution and excitation function. LIF and multi-photon techniques are most useful for sensitive, spatially resolved detection of atoms, radicals, and ions; opto-galvanic techniques can complement the LIF techniques in regions of the plasma, such as the sheaths, where LIF is unobservable; IR and Raman techniques are well suited for detection of polyatomic, non-fluorescent molecules such as the freons, which comprise the feedstock in many plasma processes.

A simple example may serve best to illustrate the as yet unfulfilled promise of optical diagnostics in the plasma processing environment. When organic materials, such as polyimide or photoresists, are etched in an O_2 plasma, anisotropy is only observed at low pressure, regardless of applied power (75,76). These observations appear to be in conflict with current theories that line profiles in ion-assisted etching are controlled primarily by the ratio of the sheath electric field to the total gas density, E_s/N (45). Since the rf power should be approximately proportional to $|E_S|^2$ (77), it is curious that anisotropic organic etching cannot be achieved at high power density and high pressure. Basically two explanations

can be offered for the discrepancy between theory and experiment. First, if an increase in rf power merely expands the plasma volume without increasing the power density, the measured rf power is no longer a measure of the sheath field. Secondly, if the sheath field and ion flux to the organic surface increase with rf power but the radical O atom flux increases by much more, then the ion-assisted chemistry, which is responsible for anisotropic etching, will become relatively less important than the neutral chemistry, which is responsible for iostropic etching. If higher anisotropic etching rates are desired, then greater control of either the ion vs. neutral chemistry or the plasma volume or both at higher pressure is required. But how can this control be achieved if we don't know which explanation is correct?

Clearly, optical techniques can come to the rescue. For example, spatially-resolved optical emission or LIF would be a good means to evaluate the plasma volume. The sheath electric field could conceivably be measured by a TDLS Stark shift or an LIF Stark intensity measurement. The concentration of O and O^+ could be measured by two-photon LIF or by emission actinometry. The O_2^+ concentration could be measured by one-photon LIF while the O_2 concentration could be measured by Raman techniques. Once such experiments were performed, the explanation for the discrepancy between theory and experiment should be obvious. Given an explanation, let us say the neutral flux increases by much more than the ion flux, we could try to achieve better process control by adding a neutral scavenger and thereby suppress the neutral-surface reaction and increase the anisotropy. The effects of adding the scavenger could be monitored in real time by the optical diagnostics described above.

Measured concentrations, fluxes, and fields in rf plasmas can be compared to results of kinetic model calculations (78,79) to obtain a better understanding of glow discharge processes. In the example cited above, it is possible that the theory would be found wanting in which case we would have improved not only our process control but also our fundamental understanding of plasma-surface chemistry.

REFERENCES

[1] W. R. Harshbarger, R. A. Porter, T. A. Miller, and P. Norton, Appl. Spectrosc. *31*, 201 (1977).

[2] C. J. Mogab, A. C. Adams, and D. L. Flamm, J. Appl. Phys. *49*, 3796 (1978).

[3] D. L. Flamm, *Solid State Technology 22*, 109 (April 1979).

[4] J. W. Coburn and M. Chen, J. Appl. Phys. *51*, 3134 (1980).

[5] R. d'Agostino, F. Cramarossa, S. DeBenedictis, and G. Ferraro, J. Appl. Phys. *52*, 1259 (1981).

[6] R. d'Agostino, V. Colaprico, and F. Cramarossa, Plasma Chem. and Plasma Proc. *1*, 365 (1981).

[7] R. d'Agostino, F. Cramarossa, V. Colaprico, and R. d'Ettole, J. Appl. Phys. *54*, 1284 (1983).

[8] R. d'Agostino, F. Cramarossa, and S. DeBenedictis, Plasma Chem. and Plasma Proc. *2*, 213 (1982).

[9] V. M. Donnelly, W. C. Dautremont-Smith, D. L. Flamm, and D. J. Werder, J. Appl. Phys. (in press).

[10] D. E. Ibbotson, D. L. Flamm, and V. M. Donnelly, J. Appl. Phys. (in press).

[11] H.-J. Tiller, D. Berg, and R. Mohr, Plasma Chem. and Plasma Proc. *1*, 247 (1981).

[12] R. A. Gottscho, G. P. Davis, and R. H. Burton, Plasma Chem. and Plasma Proc. *3*, 193 (1983); J. Vac. Sci. Technol. *A1*, 622 (1983).

[13] J. P. Simons and A. J. Yarwood, Nature *187*, 316 (1960).

[14] R. A. Gottscho, unpublished results.

[15] T. Ogawa and M. Higo, Chem. Phys. Lett. *65*, 610 (1979), and references therein.

[16] R. A. Gottscho and V. M. Donnelly, to be submitted to J. Appl. Phys.

[17] D. L. Flamm and V. M. Donnelly, Bull. Am. Phys. Soc. *27*, 97 (1982).

[18] G. Herzberg, *Molecular Spectra and Molecular Structure I. Spectra of Diatomic Molecules*, (van Nostrand Reinhold Co., New York, 1950).

[19] W. R. Harshbarger and R. A. Porter, Appl. Spectrosc. *35*, 130 (1981).

[20] R. A. Porter and W. R. Harshbarger, J. Electrochem. Soc. *126*, 460 (1979).

[21] M. Oshima, Jpn. J. Appl. Phys. *17*, 1157 (1978).

[22] S. DeBenedictis, R. d'Agostino, and F. Cramarossa, Chem. Phys. *71*, 247 (1982).

[23] G. P. Davis and R. A. Gottscho, J. Appl. Phys. *54*, 3080 (1983).

[24] D. M. Mehs and T. M. Niemczyk, Appl. Spectrosc. *35*, 66 (1981).

[25] G. Rosny, E. R. Mosburg, Jr., J. R. Abelson, G. Devand, and R. C. Kerns, J. Appl. Phys. *54*, 2272 (1983).

[26] R. A. Gottscho, R. H. Burton, D. L. Flamm, V. M. Donnelly, and G. P. Davis, to be submitted to J. Appl. Phys.

[27] A. Garscadden, "Ionization Waves in Glow Discharges," in *Gaseous Electronics Vol. 1*, ed. by M. N. Hirsh and H. Oskam, Academic Press (New York, 1978), pp. 65-107.

[28] D. L. Flamm, E. R. Gilliland, and R. F. Baddour, Ind. Eng. Chem. Fundam. *12*, 277 (1973).

[29] J. L. Kinsey, Ann. Rev. Phys. Chem. *28*, 349 (1977).

[30] V. M. Donnelly, D. L. Flamm, and G. Collins, J. Vac. Sci. Technol. *21*, 817 (1982).

[31] P. J. Hargis, Jr. and M. J. Kushner, Appl. Phys. Lett. *40*, 779 (1982).

[32] S. Pang and S. R. J. Brueck, "Laser-Induced Fluorescence Diagnostics of $CF_4/O_2/H_2$ Plasma Etching," in *Laser Diagnostics and Photochemical Processing for Semiconductor Devices*, ed. R. M. Osgood, S. R. J. Brueck, and H. R. Schlossberg, North Holland, (New York, 1983), p. 161.

[33] G. Smolinsky and D. L. Flamm, J. Appl. Phys. *50*, 4982 (1979).

[34] D. L. Flamm, Plasma Chem. and Plasma Proc. *1*, 37 (1981).

[35] E. A. Truesdale and G. Smolinsky, J. Appl. Phys. *50*, 6594 (1979).

[36] R. A. Gottscho, R. H. Burton, and G. P. Davis, J. Chem. Phys. *77*, 5298 (1982).

[37] W. E. Wentworth, R. George, and H. Keith, J. Chem. Phys. *51*, 1791 (1969).

[38] E. Schultes, A. A. Christodoulides, and R. N. Schindler, Chem. Phys. *8*, 354 (1975), and references therein.

[39] H. U. Scheunemann, E. Illenberger, H. Baumgärtel, Ber. Bunsenges. Phys. Chem. *84*, 580 (1980).

[40] L. G. Christophorou, Environ. Health Persp. *36*, 3 (1980).

[41] K. Uchino, M. Maeda, K. Koga, Y. Sonoda, K. Muraoka, and M. Akazaki, Jpn. J. Appl. Phys. *21*, 906 (1982).

[42] R. H. Bruce, Proc. Symp. Plasma Proc., ed. R. G. Frieser and C. J. Mogab, Electrochem. Soc. (St. Louis, 1980), p. 243.

[43] R. H. Bruce, J. Appl. Phys. *52*, 7064 (1981).

[44] R. E. Walkup, R. W. Dreyfus, and P. Avouris, Conf. on Lasers and Electro-Optics, May 17-20, 1983, Baltimore, Md., Abstract# TUA2, and Phys. Rev. Lett, in press (June 1983).

[45] C. B. Zarowin, J. Electrochem. Soc., *130*, 1144 (1983).

[46] C. C. Wang and D. K. Killinger, Phys. Rev. Lett. *39*, 929 (1977).

[47] C. R. Webester and C. T. Rettner, Laser Focus, 41 (Feb. 1983).

[48] J. C. Knights, J. P. M. Schmitt, J. Perrin, and G. Guelachvili, J. Chem. Phys. *76*, 3414 (1982).

[49] H. Sakai, P. Hansen, M. Esplin, R. Johansson, M. Peltola, and J. Strong, Appl. Opt. *21*, 228 (1982).

[50] H. U. Poll, D. Hinze, and H. Schlemm, Appl. Spec. *36*, 445 (1982).

[51] C. Yamada and E. Hirota, J. Mol. Spectrosc. *74*, 203 (1979).

[52] K. Matsumara, K. Kawaguchi, K. Nagai, C. Yamada, and E. Hirota, J. Mol. Spectrosc. *84*, 68 (1980).

[53] C. Yamada, K. Nagai, and E. Hirota, J. Mol. Spectrosc. *85*, 416 (1981).

[54] C. A. DeJoseph, Jr., A. Garscadden, and D. R. Pond, Proc. Lasers 1982 (New Orleans, 1982).

[55] A. C. Stanton and C. E. Kolb, J. Chem. Phys. *72*, 6637 (1980).

[56] P. B. Davies and D. K. Russell, Chem. Phys. Lett. *67*, 440 (1979).

[57] N. N. Haese, F. Pan, and T. Oka, Phys. Rev. Lett. *50*, 1575 (1983).

[58] C. S. Gudeman, M. H. Begemann, J. Pfaff, and R. J. Saykally, Phys. Rev. Lett. *50*, 727 (1983).

[59] C. S. Gudeman, M. H. Begemann, J. Pfaff, and R. J. Saykally, J. Chem. Phys. *78*, 5837 (1983).

[60] L. A. Farrow and R. E. Richton, unpublished.

[61] B. S. Choi and H. Kim, Appl. Spectrosc. *36*, 71 (1982), and references therein.

[62] M. Deutsch and I. Beniaminy, J. Appl. Phys. *54*, 137 (1983), and references therein.

[63] J. C. Cummings and D. P. Aeschliman, Opt. Comm. *31*, 165 (1979).

[64] D. S. Moore, Chem. Phys. Lett. *89*, 131 (1982).

[65] A. C. Eckbreth and P. Schreiber, *Chemical Applications of Nonlinear Raman Spectroscopy*, ed. A. B. Harvey, Academic Press (New York, 1981), Chapter 2.

[66] Spontaneous Raman scattering has also been used to detect oxygen atoms in high pressure flames by J. Dasch and J. H. Bechtel, Opt. Lett. *6*, 36 (1981).

[67] N. Hata, A. Matsuda, K. Tanaka, K. Kajiyama, N. Moro, and K. Sajiki, Jpn. J. Appl. Phys. *22*, L1 (1983).

[68] P. J. Hargis, Jr., Appl. Opt. *20*, 149 (1981).

[69] A. V. Voskanyan, S. B. Leonov, V. E. Mitsuk, and Y. A. Rusanov, Sov. Tech. Phys. Lett. *7*, 481 (1981).

[70] J. Bokor, R. R. Freeman, J. C. White, R. H. Storz, Phys. Rev A *24*, 612 (1981).

[71] W. K. Bischel, B. E. Perry, and D. R. Crosley, Chem. Phys. Lett. *82*, 85 (1981) and Appl. Opt. *21*, 1419 (1982).

[72] M. Alden, H. Edner, P. Grafstrom, and S. Svanberg, Opt. Comm. *42*, 244 (1982).

[73] P. Brewer, N. Van Veen, and R. Bersohn, Chem. Phys. Lett. *91*, 126 (1982).

[74] M. Heaven, T. A. Miller, R. R. Freeman, J. White, and J. Bokor, Chem. Phys. Lett. *86*, 458 (1982).

[75] F. Y. Robb, Electrochem. Soc. Meeting, San Francisco, Ca., May 8-13, 1983, abstract# 176.

[76] B. R. Soller, R. F. Shuman, and R. R. Ross, Electrochem. Soc. Meeting, San Francisco, Ca., Abstract# 180.

[77] C. B. Zarowin and R. S. Howath, J. Electrochem. Soc. *129*, 2541 (1982).

[78] M. J. Kushner, J. Appl. Phys. *53*, 2923 (1982).

[79] D. Edelson and D. L. Flamm, 7th International Symposium on Gas Kinetics, Aug. 23-27, 1982, Göttingen, Germany, Abs.# D48.